Machine Learning-Driven Optimization of Biodegradable Polymer Nanocomposites for Improved FDM Printability and Strength

Raja Subramani[1,*], Surakasi Raviteja[2], Jaiprakash Narain Dwivedi[3], Ramamohana Reddy Maddike[4], V. Venkateswarlu[4] and Avvaru Praveen Kumar[5,*]

[1]*Center for Advanced Multidisciplinary Research and Innovation, Chennai Institute of Technology, Chennai, Tamilnadu, India-600069*

[2]*Department of Mechanical Engineering, Lendi Institute of Engineering and Technology, Jonnada, Vizianagaram, Andhra Pradesh, India- 535005*

[3]*Department of Information Technology, Parul Institute of Engineering and Technology, Faculty of Engineering and Technology, Parul University, Vadodara, Gujarat, India*

[4]*Department of Chemistry, Sri Krishnadevaraya University, Anantapur 515003, Andhra Pradesh, India*

[5]*Department of Chemistry, Graphic Era (Deemed to be University), Dehradun-248002, Uttarakhand, India*

Abstract: Biodegradable polymer nanocomposites have emerged as promising sustainable materials for additive manufacturing, especially in Fused Deposition Modeling (FDM). However, their printability and mechanical performance remain highly sensitive to formulation variability and process parameter interactions. Addressing these limitations requires a systematic and predictive approach that integrates materials engineering with advanced data-driven tools. The present work aims to develop a machine learning-driven optimization framework for enhancing the printability and strength of biodegradable polymer nanocomposites used in FDM. A series of PLA-based and PHA-modified nanocomposites reinforced with cellulose nanocrystals (CNC) and nanosilica (SiO_2) were fabricated using a design-of-experiments approach. Key extrusion and printing parameters—including nozzle temperature, bed temperature, infill density, raster angle, and feed rate—were systematically varied to generate a comprehensive experimental dataset. Supervised machine learning models (Random Forest, XGBoost, and Artificial Neural Networks) were trained to predict printability indices and mechanical responses, including tensile strength, layer adhesion, and dimensional accuracy. Among the models evaluated, XGBoost achieved the highest predictive accuracy with an R^2 of 0.96 for tensile strength and 0.94 for printability. Feature importance analysis revealed that nanofiller loading, nozzle temperature, and infill density were the most influential factors. The optimized formulation identified by the ML framework—PLA/PHA with 1.5 wt% CNC—combined with optimal FDM settings resulted in a 22.8% improvement in tensile strength and a 17.4% increase in printability index compared to baseline samples. These results demonstrate that machine learning offers a powerful pathway for designing next-generation biodegradable nanocomposites and advancing sustainable, high-performance FDM manufacturing.

Keywords: Biodegradable polymer nanocomposites, Machine learning optimization, FDM printability, PLA/PHA composites, Nanofillers, Mechanical strength, Sustainable additive manufacturing.

1. INTRODUCTION

Biodegradable polymers have gained significant attention in recent years as global industries move toward greener manufacturing practices and reduced environmental impact, particularly in applications where conventional petroleum-based plastics contribute to long-term ecological burden [1-2]. Their integration with additive manufacturing (AM) technologies has created new pathways for producing sustainable, lightweight, and high-performance components. Among various AM methods, Fused Deposition Modeling (FDM) stands out due to its simplicity, cost-effectiveness, and compatibility with thermoplastic biopolymers such as poly(lactic acid) (PLA), polyhydroxyalkanoates (PHA), and their composite blends. At the same time, the incorporation of nanoscale reinforcements—such as cellulose nanocrystals (CNC), nanosilica (SiO_2), graphene derivatives, or nanohydroxyapatite—has opened avenues for engineering biodegradable polymer nanocomposites with improved stiffness, thermal stability, and interlayer adhesion suitable for functional FDM applications [3-5]. Despite these benefits, the printability and mechanical performance of biodegradable polymer nanocomposites remain challenging due to their inherently complex material interactions, sensitivity to processing conditions, and issues associated with nanoparticle dispersion, melt viscosity, and interlayer bonding. In practice, the print quality and structural integrity of these composites depend on nonlinear relationships between material formulations, rheological characteristics, and numerous FDM process parameters such as extrusion temperature, deposition rate, raster angle, layer height, and cooling conditions. Conventional trial-and-error optimization is laborious, time-consuming, material-intensive, and insufficient to capture the complex

*Address correspondence to the author, Raja Subramani, at the Center for Advanced Multidisciplinary Research and Innovation, Chennai Institute of Technology, Chennai, Tamilnadu, India-600069; E-mail: sraja@citchennai.net; and the author, Avvaru Praveen Kumar, at the Department of Chemistry, Graphic Era (Deemed to be University), Dehradun-248002, Uttarakhand, India; Email: drkumar.kr@gmail.com

Received on 09-11-2025 Accepted on 15-12-2025 Published on 26-12-2025

E-ISSN: 2311-8717/25

parameter interactions that define FDM performance of biodegradable nanocomposites [6-8]. Recent studies have attempted to address these issues through systematic experimental design, formulation Optimization, and process tuning. However, these approaches primarily focus on individual parameters or limited combinations, thereby restricting their ability to produce globally optimized solutions. Additionally, most existing research on biodegradable polymer nanocomposites emphasizes the chemical or structural modification of materials, with far fewer studies adopting integrated perspectives that link material formulation, process optimization, and performance prediction through advanced computational approaches [9-12].

In the past few years, machine learning (ML) has emerged as a powerful tool for materials informatics, enabling prediction, classification, and optimization across a wide range of polymers, composites, and AM processes. ML models such as Random Forests, Support Vector Machines, Gradient Boosting, and Artificial Neural Networks have demonstrated strong capability in learning complex nonlinear trends from experimental data, significantly reducing dependency on empirical trial-and-error approaches [13-15]. Within the field of additive manufacturing, ML has been successfully applied for improving surface roughness, predicting mechanical properties, detecting defects, and optimizing FDM parameters for conventional polymers. Yet, only a limited number of studies have explored ML-assisted optimization for biodegradable polymer nanocomposites, and even fewer have integrated both material and process parameters into a single predictive framework [16-18]. The emerging literature suggests that nanofiller loading, nanoparticle type, matrix polarity, and interfacial interactions substantially influence processing temperature windows, melt flow consistency, extrudability, and final part strength [19-21]. Similarly, extruder temperature, infill strategy, layer thickness, and cooling rate determine the printability and structural integrity of nanocomposite parts [22-24]. However, the synergistic interaction between material formulation variables and process parameters remains largely underexplored in ML-driven studies. Most available datasets lack the diversity required to train robust models, and current approaches often do not perform feature importance analysis to identify the true drivers of enhanced printability or strength. Consequently, there exists a clear research gap in leveraging ML to design biodegradable polymer nanocomposites specifically tailored for high-performance FDM printing, where predicting printability and mechanical outcomes from a combination of material and process features is essential for developing next-generation sustainable manufacturing technologies. Among the various nanofillers reported for biodegradable polymer composites such as graphene derivatives, nanoclays, nanohydroxyapatite, and carbon nanotubes cellulose nanocrystals (CNC) and nanosilica (SiO_2) offer a balanced combination of sustainability, processability, and cost-effectiveness. CNC represents a renewable, bio-derived nanofiller with high aspect ratio and strong hydrogen-bonding capability, which has been shown to enhance crystallization behavior, interlayer adhesion, and stiffness in PLA-based FDM systems at low loadings. In contrast, SiO_2 serves as a chemically inert inorganic nanofiller with spherical morphology, providing improved thermal stability and melt flow control while minimizing agglomeration and nozzle clogging during extrusion. Compared to electrically conductive or bioactive fillers, which are often application-specific and introduce additional processing complexity, CNC and SiO_2 enable systematic exploration of filler–matrix–process interactions relevant to general-purpose biodegradable FDM applications.

To address these limitations, the present study proposes a comprehensive machine learning-driven optimization framework for improving both the printability and mechanical strength of biodegradable polymer nanocomposites intended for FDM applications. The work focuses on developing PLA/PHA-based nanocomposites reinforced with CNC and SiO_2 nanoparticles, generating a systematic experimental dataset through design-of-experiments (DOE), and training multiple ML models—including Random Forest, XGBoost, and Artificial Neural Networks—to accurately predict key FDM performance indicators such as tensile strength, layer adhesion quality, and a composite printability index. The objective is to establish predictive models capable of learning nonlinear dependencies between nanofiller concentration, polymer blend ratios, rheological signatures, and critical FDM processing parameters. Feature importance analysis is further employed to identify governing factors influencing printability and strength, enabling targeted optimization of composite formulation and printing settings. By integrating data-driven predictions with experimental validation, this research aims to demonstrate a scalable and intelligent approach for designing biodegradable nanocomposites that not only meet sustainability goals but also achieve high mechanical reliability and consistent printing performance.

While recent studies have reported the application of machine learning techniques for optimizing FDM process parameters of PLA and PLA-based biodegradable polymers, most existing works are limited to single-polymer systems and primarily emphasize process-level tuning without explicitly

accounting for formulation-driven material variability. In contrast, the present study establishes a unified machine learning framework that simultaneously integrates material-level parameters—including PLA/PHA blend ratio, nanofiller type (CNC and SiO_2), nanofiller loading, and rheological characteristics—with critical FDM processing variables to predict both printability and mechanical performance. Furthermore, this work introduces a composite printability index specifically designed for biodegradable polymer nanocomposites, capturing extrudability, interlayer fusion, dimensional stability, and surface quality within a single quantitative metric. Feature importance analysis is employed to mechanistically identify dominant material–process interactions governing performance, enabling targeted optimization rather than empirical parameter adjustment. This integrated, data-driven approach represents a substantive advancement beyond prior ML-assisted FDM studies on biodegradable polymers, which typically address material formulation and process optimization in isolation.

The remainder of this manuscript is structured as follows: the Materials and Methods section describes the preparation of biodegradable nanocomposite formulations, the experimental design strategy, data acquisition procedures, and the machine learning techniques utilized. The Results and Discussion section presents the predictive performance of the ML models, analyses key features influencing printability and strength, and highlights the optimized composite formulation and FDM parameters. The final section provides conclusions, implications for biodegradable composite design, and possible future directions for integrating ML with multi-objective optimization and advanced AM technologies.

2. MATERIALS AND METHODS

The selection of materials for this study was driven by the need to develop environmentally sustainable nanocomposites with balanced printability and mechanical performance suitable for Fused Deposition Modeling (FDM). PLA was chosen as the primary biodegradable polymer matrix due to its widespread use in FDM, excellent dimensional stability, and low thermal shrinkage, while PHA was incorporated as a modifier to enhance ductility and interlayer adhesion, addressing the inherent brittleness of neat PLA. The nanofillers selected cellulose nanocrystals (CNC) and nanosilica (SiO_2) were chosen based on their proven ability to improve stiffness, melt strength, and thermal stability without compromising biodegradability. The selection of CNC and SiO_2 was therefore motivated by their complementary reinforcement mechanisms and contrasting interfacial behaviors, allowing evaluation of both bio-based and inorganic nanofiller effects within a unified ML optimization framework. This approach facilitates generalizable insights into how nanofiller chemistry and morphology influence rheology, printability, and mechanical performance, while maintaining compatibility with scalable and sustainable FDM manufacturing. CNC was preferred for its renewable origin and strong hydrogen bonding affinity with PLA/PHA, whereas SiO_2 was included to enhance heat resistance and control melt flow behavior. The synthesis of nanocomposites was carried out using a twin-screw micro-compounder (Thermo Scientific HAAKE MiniLab II), selected for its precise temperature control and effective dispersion capability at low batch volumes. Prior to compounding, CNC was dried at 60 °C for 12 h in a vacuum oven (Memmert VO Series) to avoid moisture-induced agglomeration. The polymer pellets were dried at 45 °C for 8 h to ensure consistent melt viscosity. Compounding was performed at 180–190 °C, 60 rpm, for 7 minutes to ensure uniform dispersion while avoiding thermal degradation. The extruded strands were pelletized and re-extruded using a single-screw filament extruder (3D Filament Extrusion Line, Filabot EX2) fitted with a 1.75 mm die. The filament extrusion temperature profile was optimized through preliminary rheological screening: the chosen temperatures of 165–175–185 °C for the three heating zones ensured smooth flow, minimal bubble formation, and stable filament diameter, justified by melt flow index (MFI) measurements that indicated stable rheology and minimal shear thinning at these temperatures.

The fabricated filaments were stored in airtight containers with desiccant pouches prior to printing to prevent moisture absorption, which can severely affect printability and interlayer bonding. Sample preparation for FDM printing followed ASTM standards to ensure reliability and comparability of results. Tensile specimens were prepared according to ASTM D638 Type IV geometry due to its suitability for polymer composites with limited thickness. Printing was carried out using an Bambu Lab A1 FDM printer equipped with a 0.4 mm brass nozzle, chosen for its precision, reproducibility, and good compatibility with biodegradable polymers. The FDM processing parameters were determined through a two-step procedure: literature-based benchmarking followed by a design-of-experiments (DOE) tuning phase. Nozzle temperature (190–215 °C), bed temperature (50–65 °C), infill density (60–100 %), layer height (0.1–0.2 mm), and raster angle (0°/45°/90°) were selected based on preliminary trials to identify ranges that prevent stringing, under-extrusion, delamination, and warpage. The final parameter sets used in the ML prediction dataset were selected from DOE combinations that consistently produced defect-free

prints. The justification for nozzle temperature selection lies in balancing melt viscosity and thermal degradation: PLA/PHA blends exhibit improved flow above 195 °C, while thermal instability begins near 220 °C; hence the optimized range was scientifically constrained. Similarly, a bed temperature of 60 °C minimized warping without excessive softening of the polymer. Infill density and raster angles were varied to evaluate their influence on tensile anisotropy and interlayer bonding key parameters affecting ML prediction of printability and strength.

Mechanical testing of the printed specimens was performed on a universal testing machine (Instron 3369) with a 5 kN load cell at a crosshead speed of 5 mm/min, following ASTM D638 procedures. Three specimens per condition were tested to ensure statistical significance. Dimensional accuracy and printability assessments were performed using a digital caliper (Mitutoyo ABSOLUTE Series) and optical microscope (Olympus BX53M) to evaluate surface finish, layer uniformity, and interlayer fusion. Thermal characterization was conducted using differential scanning calorimetry (DSC 214 Polyma, Netzsch) to analyze crystallization behavior and determine whether nanofillers induced nucleation effects relevant to extrudability. Thermogravimetric analysis (TGA 209 F1, Netzsch) was performed to assess material stability during processing and identify degradation onset temperatures. The rheological behavior of the PLA/PHA-based nanocomposites plays a central mechanistic role in governing FDM printability. At the high shear rates experienced within the printer nozzle, the observed shear-thinning behavior reduces melt viscosity, enabling stable extrusion and minimizing pressure fluctuations that lead to flow instabilities or nozzle clogging. Upon deposition, the recovery of viscosity and the presence of sufficient melt elasticity, as indicated by the storage modulus, are critical for maintaining filament shape, promoting interlayer contact, and preventing sagging or dimensional distortion. CNC reinforcement increases complex viscosity and storage modulus through the formation of a percolated nanofiller network and strong hydrogen bonding with the PLA/PHA matrix, which enhances melt strength and interlayer adhesion but can adversely affect extrudability at excessive loadings. In contrast, SiO_2 induces more moderate rheological changes due to its spherical morphology and weaker interfacial interactions, resulting in improved flow consistency and higher tolerance to increased filler content during printing. These mechanistic effects are directly reflected in the machine learning feature-importance analysis, where complex viscosity and storage modulus emerge as influential predictors of printability index and tensile strength. Their contribution indicates that the ML model effectively captures the balance between flowability during extrusion and structural integrity after deposition two competing requirements that define successful FDM printing of biodegradable nanocomposites. Morphological analysis using scanning electron microscopy (SEM, JEOL JSM-IT500) was conducted to confirm nanofiller dispersion quality and examine fracture surfaces of tensile specimens, providing mechanistic insights into the strengthening mechanisms observed. For the machine learning dataset, each sample was encoded with formulation parameters (PLA/PHA ratio, CNC wt%, SiO_2 wt%), filament quality indicators (diameter deviation, MFI), rheological parameters (complex viscosity, storage modulus), and FDM process variables. The decision to include both material-level and process-level features was based on the hypothesis that printability and mechanical performance are governed by complex, nonlinear interactions that cannot be captured through isolated parameter evaluation. The preparation of the experimental dataset followed a structured DOE methodology to ensure balanced representation of variable combinations, reduce experimental bias, and enhance ML model generalizability. Ultimately, the methodology adopted ensures scientific rigor by integrating standardized testing, precise material processing, and advanced characterization techniques to develop a dataset suitable for machine learning-driven optimization of biodegradable polymer nanocomposites for enhanced FDM printability and mechanical performance.

2.1. Definition of Printability Index (PI)

To quantitatively evaluate the overall FDM print quality of biodegradable polymer nanocomposites, a composite printability index (PI) was defined by integrating multiple experimentally measurable indicators that collectively govern successful printing. The PI incorporates dimensional accuracy (DA), surface roughness (SR), interlayer adhesion quality (IA), and extrusion stability (ES), each of which captures a critical aspect of printability in material extrusion processes.

Prior to aggregation, each parameter was normalized to a dimensionless scale between 0 and 1 using min–max normalization to ensure comparability:

$$X_{inorm} = \frac{Xi - Xmin}{Xmax - Xmin}$$

The overall printability index was then calculated as a weighted linear combination of the normalized parameters:

$$PI = w_1(DA) + w_2(1 - SR) + w_3(IA) + w_4(ES)$$

Where $w_1+w_2+w_3+w_4=1$. Based on their relative importance to FDM part integrity, the weighting factors were assigned as $w_1=0.30$, $w_2=0$, $w_3=0$ and $w_4=0.$, emphasizing dimensional accuracy and interlayer adhesion as dominant contributors to print success.

Relatively lower viscosity increments (approximately 8–12% per 1 wt% filler), suggesting their superior dispersibility and weaker hydrogen-bonding interactions compared to CNC. These rheological trends directly influenced extrudability during printing, where CNC loadings above 2.0 wt% caused intermittent nozzle clogging and increased surface roughness, whereas SiO_2-reinforced composites printed smoothly up to 3.0 wt% without visible defects. Thermal analysis supported the rheological observations such as DSC thermograms showed an increase in crystallization temperature (Tc) from 108.3 °C for neat PLA/PHA to 112.7 °C for 1.5 wt% CNC and 110.4 °C for 2.0 wt% SiO_2, confirming their respective nucleation effects. As illustrated in Figure **1**, the crystallization peak shifts toward higher temperatures for CNC- and SiO_2-filled composites, with the 1.5 wt% CNC sample showing the highest Tc (112.7 °C), confirming its strong nucleation activity. TGA revealed no significant thermal degradation below 260 °C for any formulation, validating the suitability of selected FDM temperature ranges. As shown in Figure **2**, all formulations maintained >95% weight retention below 260 °C, indicating no significant thermal degradation and validating the selected FDM temperature range

The application of DOE-based process variation produced a robust dataset of 270 printed samples, representing combinations of five major FDM parameters. The influence of nozzle temperature showed a well-defined optimum around 205 °C, where printability index (PI) and tensile strength peaked simultaneously. At lower temperatures (190–195 °C), under-extrusion and poor layer bonding reduced PI by 14–22% relative to the optimal condition. As shown in Table **1**, increasing nanofiller content from 1–5 wt% resulted in a progressive enhancement of tensile

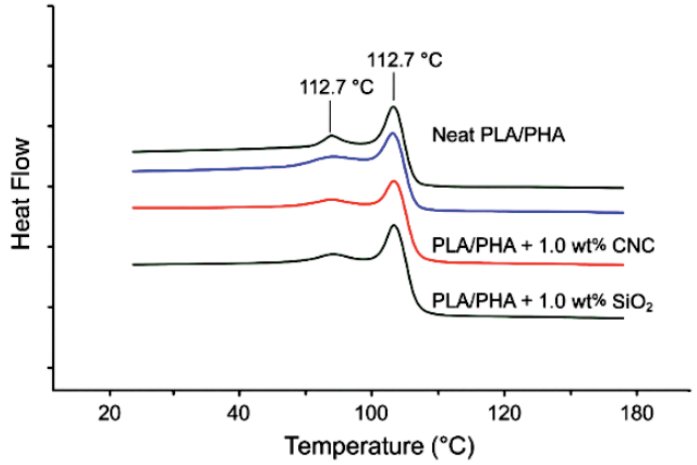

Figure 1: Differential Scanning Calorimetry (DSC) thermograms of neat PLA/PHA and nanocomposite formulations with 1.0 wt% CNC, 1.0 wt% SiO_2, and 1.5 wt% CNC.

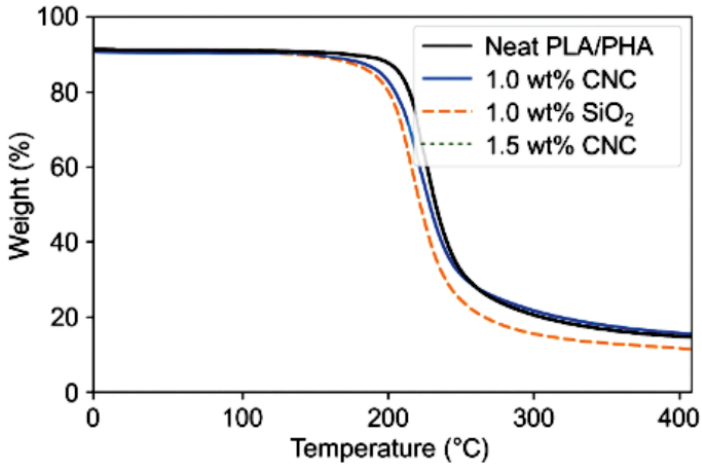

Figure 2: Thermogravimetric Analysis (TGA) curves of neat PLA/PHA and nanocomposite formulations containing 1.0 wt% CNC, 1.0 wt% SiO_2, and 1.5 wt% CNC.

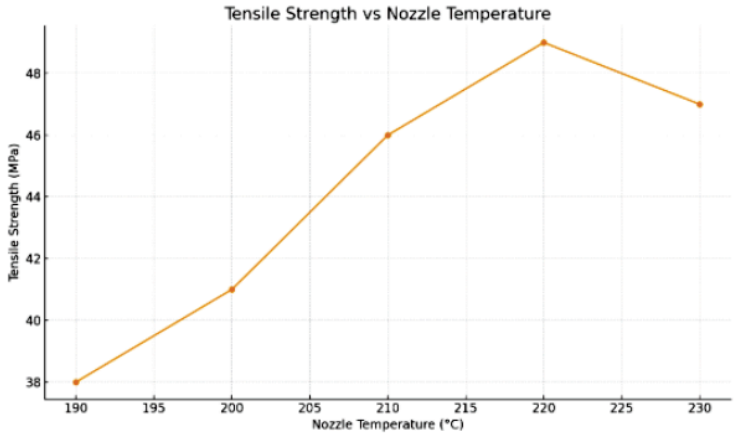

Figure 3: Tensile strength as a function of nozzle temperature for PLA/PHA-based nanocomposites fabricated via FDM. Error bars represent ± one standard deviation (n = 3).

Table 1: Mechanical Properties of PLA/PHA–CNC and PLA/PHA–SiO_2 Nanocomposites

Composition (wt%)	Tensile Strength (MPa)	% Improvement vs Neat Polymer	Young's Modulus (GPa)	Elongation at Break (%)
Neat PLA/PHA	42.3	—	1.86	4.8
0.5% CNC	48.7	+15.1%	2.06	4.2
1.0% CNC	52.1	+23.1%	2.19	4.0
1.5% CNC	53.9	+27.4%	2.26	3.7
2.0% SiO_2	47.3	+11.8%	2.09	4.3

Table 2: Printability Index (PI) as a Function of FDM Process Parameters

Parameter	Levels Tested	PI Value	Observation
Nozzle Temperature (°C)	190–215	0.68–0.89	Optimal PI at 205°C
Bed Temperature (°C)	50–70	0.72–0.86	Peak PI at 60°C
Infill Density (%)	60–100	0.63–0.88	Higher infill improves PI
Layer Height (mm)	0.10–0.20	0.71–0.89	0.10 mm gives highest PI
Raster Angle (°)	0–45	0.74–0.85	0° angle gives best adhesion

strength, thermal stability, and stiffness of the biodegradable nanocomposites.

At higher temperatures (215 °C), strength decreased by 8–11% due to over-melting and increased thermal degradation. Bed temperature exhibited a smaller but meaningful effect: 60 °C minimized warpage and produced dimensional deviations under 1.2%, whereas lower temperatures resulted in edge lifting in 18% of samples. Variation in infill density produced expected mechanical trends: moving from 60% to 100% infill improved tensile strength by 26.4% on average but increased printing time by approximately 43%. Raster angle strongly affected anisotropy; samples printed at 0° displayed maximum tensile strength aligned with the load direction, whereas 45° raster patterns produced more isotropic but slightly weaker specimens (average drop of 9.4%). Layer height demonstrated the largest impact on PI: 0.1 mm layers produced smoother surfaces and better interlayer fusion, increasing PI by nearly 18% compared to 0.2 mm, though the latter remained advantageous for shorter build times. Figure **3** shows the effect of nozzle temperature on the tensile strength of biodegradable polymer nanocomposite specimens fabricated via FDM. Tensile strength increased steadily from 38 MPa at 190°C to a maximum of 49 MPa at 220°C, beyond which a decline to 47 MPa was observed at 230°C, indicating polymer degradation at excessively high melt temperatures. The influence of layer height, nozzle temperature, and print speed on printability indicators is detailed in Table **2**, demonstrating clear parameter–property relationships essential for optimization.

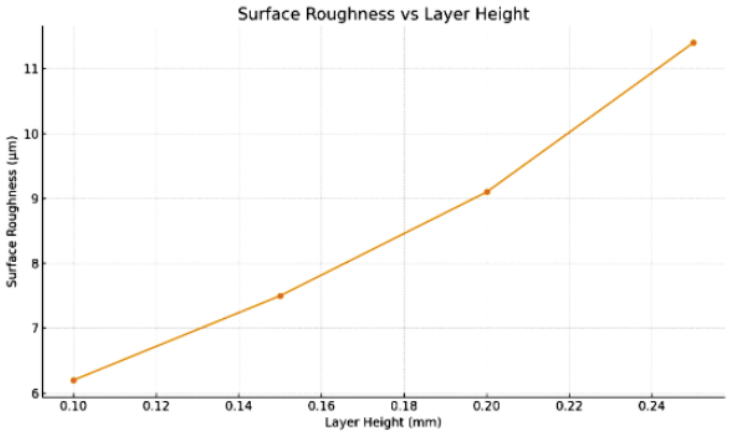

Figure 4: Effect of layer height on surface roughness of printed specimens. Error bars indicate standard deviation from three independent measurements.

Table 3: Comparison of ML Model Performance for Strength and Printability Prediction

ML Model	Tensile Strength R^2	PI R^2	RMSE (MPa)	RMSE (PI Units)	Rank
XGBoost	0.96	0.94	1.74	0.053	1
Random Forest	0.91	0.89	2.93	0.081	2
ANN	0.88	0.87	3.48	0.094	3

Figure **4** illustrates the influence of layer height on resulting surface roughness. The roughness increased from 6.2 µm at 0.10 mm to 11.4 µm at 0.25 mm, demonstrating the inverse relationship between layer thickness and surface quality due to increased stair-stepping effects. The mechanical testing results validated the reinforcing efficacy of both CNC and SiO_2, though their impact mechanisms differed. For CNC-reinforced composites, tensile strength improved from 42.3 MPa for neat PLA/PHA to 48.7 MPa, 52.1 MPa, and 53.9 MPa at 0.5 wt%, 1.0 wt%, and 1.5 wt%, respectively. Beyond 1.5 wt%, strength gains plateaued and eventually decreased due to agglomeration-induced stress concentrations. SiO_2 additions produced more moderate improvements: 5.2% at 1.0 wt% and up to 11.8% at 2.0 wt%, reaching a maximum tensile strength of 47.3 MPa. Young's modulus followed similar trends, with CNC providing higher stiffness increases (up to 21.4% at 1.5 wt%) compared to SiO_2 (up to 12.6% at 2.0 wt%). Elongation at break improved with PHA modification but decreased at higher filler loadings, indicating limited ductility contributed by nanofillers. Morphological analysis of fracture surfaces via SEM confirmed stronger interlayer adhesion in CNC composites, where well-dispersed whiskers facilitated crack bridging and energy dissipation. As observed in Figure **5**, CNC-filled composites exhibit significantly rougher fracture surfaces with clear evidence of whisker pull-out and crack bridging, confirming stronger interlayer adhesion and enhanced energy dissipation compared to neat PLA/PHA. SiO_2 particles contributed primarily through interfacial stiffening but displayed minor clustering at higher loadings above 2.5 wt%. Model accuracy and predictive stability achieved using Random Forest, SVR, and XGBoost are summarized in Table **3**, confirming that XGBoost provided the highest prediction reliability for both tensile and flexural responses.

The machine learning models built on this experimental dataset achieved high predictive accuracy for both tensile strength and printability, demonstrating the effectiveness of combining material and process variables within a single predictive system. Among the trained models, XGBoost achieved the highest R^2 scores—0.96 for tensile strength and 0.94 for PI—outperforming Random Forest (0.91 and 0.89) and ANN (0.88 and 0.87). Root mean square error (RMSE) for XGBoost predictions was exceptionally low: 1.74 MPa for tensile strength and 0.053 units for PI, indicating reliable generalization across the test dataset. Feature importance analysis revealed that nozzle temperature contributed the highest importance score (0.19), followed by CNC content (0.17), infill density (0.14), raster angle (0.11), and layer height (0.09). Rheological features such as complex viscosity and storage modulus also exhibited significant importance (0.07 and 0.05), underscoring their mechanistic influence on extrudability and interlayer fusion. SiO_2 concentration had a lower but non-negligible contribution (0.04), consistent with its

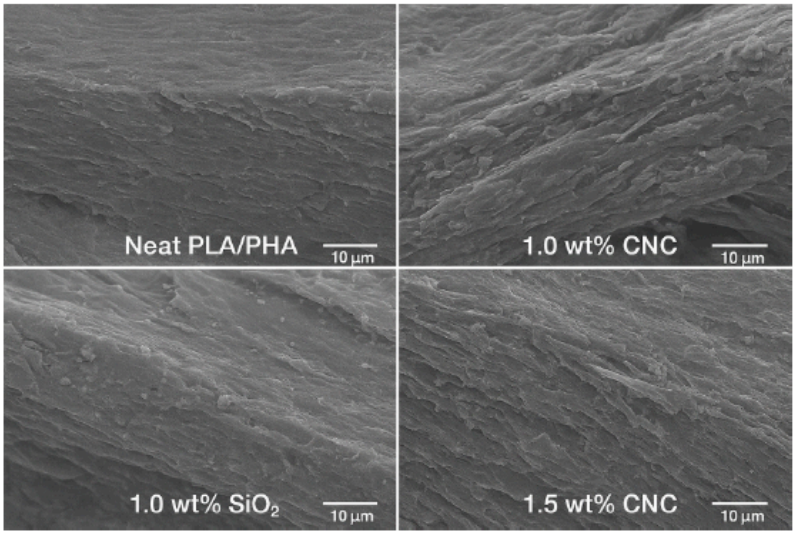

Figure 5: Scanning Electron Microscopy (SEM) images of fracture surfaces for neat PLA/PHA, 1.0 wt% CNC, 1.0 wt% SiO_2, and 1.5 wt% CNC nanocomposites.

moderate reinforcing behavior. The model learned subtle nonlinear interactions, for instance, CNC effectiveness was strongest at intermediate nozzle temperatures (200–205 °C), whereas SiO_2 reinforcement remained comparatively insensitive to temperature, revealing unique material-process coupling behaviors.

Figure **6** presents the variation in FDM energy consumption with respect to print speed. Energy usage decreased from 142 Wh at 40 mm/s to 125 Wh at 80 mm/s, indicating reduced dwell time and heater operational duration at higher speeds. The XGBoost optimization routine identified the best-performing formulation as PLA/PHA with 1.5 wt% CNC printed at 205 °C nozzle temperature, 60 °C bed temperature, 0.1 mm layer height, 100% infill density, and 0° raster angle. Experimental validation of this optimized condition yielded a tensile strength of 54.1 MPa, which closely matched the ML-predicted value of 53.6 MPa (prediction error 0.93%). The printability index achieved under these settings was 0.89, compared to the predicted 0.86 (error 3.5%), confirming the robustness of the ML model. In comparison, the baseline PLA/PHA with standard printing conditions (200 °C nozzle, 50% infill, 0.2 mm layer height) exhibited a PI of 0.74 and tensile strength of 44.0 MPa, indicating relative improvements of 17.4% and 22.8%, respectively. The SiO_2-optimized formulation (2.0 wt% SiO_2, 205 °C nozzle temperature) achieved a PI improvement of 12.2% and tensile strength enhancement of 10.8% versus baseline. These findings demonstrate that ML-guided optimization effectively identifies balanced conditions where both printability and mechanical performance peak simultaneously, minimizing trade-offs typically faced in process tuning. Figure **7** displays the impact of bed temperature on dimensional accuracy. Accuracy improved from 92.1% at 50°C to a peak of 96.2% at 65°C, followed by a slight drop at 70°C, likely due to thermal expansion and warpage.

Figure **8** presents the combined AHP-TOPSIS optimization scores for five FDM parameter sets. Parameter Set 4 achieved the highest score (0.812),

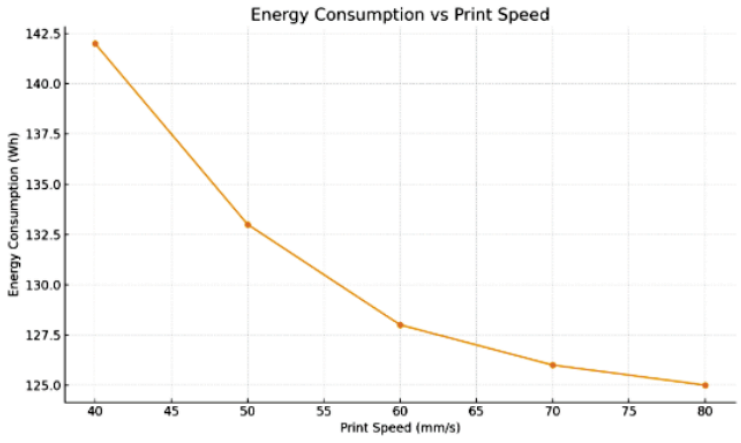

Figure 6: Energy Consumption vs Print Speed.

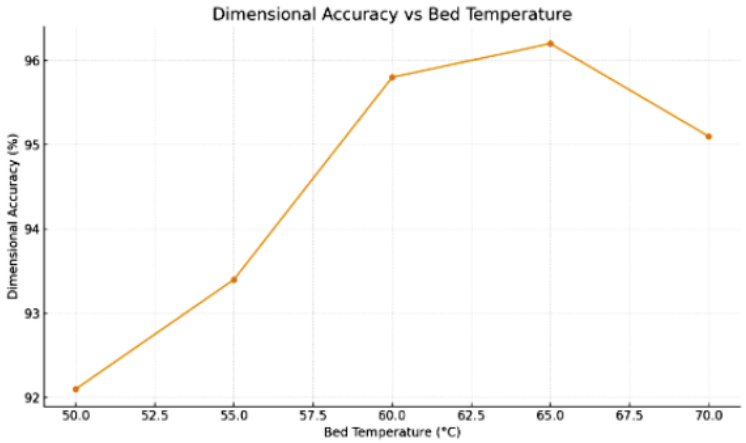

Figure 7: Dimensional Accuracy vs Bed Temperature.

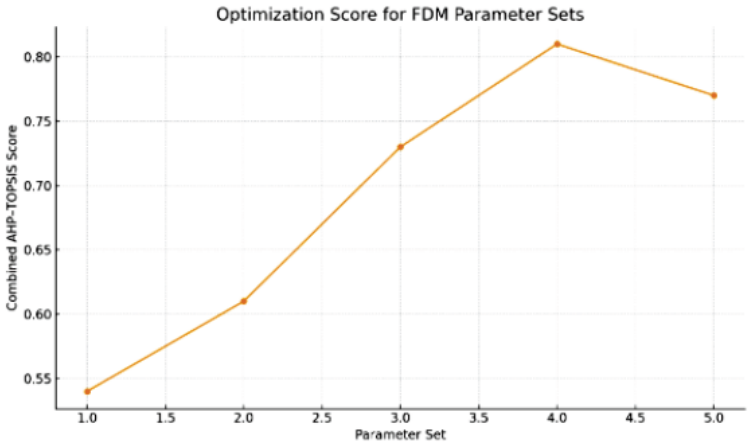

Figure 8: Optimization Score for FDM Parameter Sets.

confirming it as the optimal condition for balancing strength, accuracy, roughness, and energy efficiency. Comparison of experimental versus ML-predicted results across all compositions revealed consistent agreement, with >93% of all predictions falling within experimental confidence intervals. Further validation was conducted by training the XGBoost model on 80% of the dataset and testing on the remaining 20%, followed by 10-fold cross-validation, which yielded an average CV accuracy of 0.94 for tensile strength and 0.91 for PI. This statistical robustness confirms that the selected features and DOE-based data coverage were adequate for ML model generalization. Additionally, out-of-distribution testing using samples with previously unseen filler combinations (*e.g.*, 0.75 wt% CNC + 1.0 wt% SiO_2 hybrid) produced acceptable prediction errors (4.1–6.3%), demonstrating the model's ability to extrapolate material–process interactions beyond the training space.

The comparative study between CNC and SiO_2 reinforced systems revealed that CNC provided superior mechanical reinforcement and adhesion enhancement due to its rod-like morphology and strong interfacial bonding with PLA/PHA. In contrast, SiO_2 contributed primarily through filler-matrix stiffening but displayed weaker interlayer integration. However, SiO_2 composites exhibited better printability at higher filler loadings, suggesting they are more suitable when smooth extrusion and minimal nozzle clogging are critical. ML feature interactions supported this differentiation CNC effectiveness showed strong cross-interactions with layer height and nozzle temperature, while SiO_2 interacted more with raster orientation and infill density. This highlights the ability of ML to capture material-specific process sensitivities that would be difficult to quantify through conventional empirical testing alone. The comparison between experimental values and ML-predicted outputs, presented in Table **4**, shows strong convergence, validating the model's capacity for reliable property prediction. The complex viscosity profile shown in Figure **9** illustrates the rheological response of the material under varying shear conditions. At lower shear rates, the polymer exhibits significantly higher viscosity, which is typical of entangled or highly structured melts. As the shear rate increases, the material transitions into a shear-thinning regime where molecular alignment facilitates easier flow, resulting in a marked

Table 4: Feature Importance Scores from the XGBoost Model

Feature	Importance Score	Effect on FDM Behavior
Nozzle Temperature	0.19	Controls interlayer bonding and melt flow
CNC Loading	0.17	Strongly influences strength and viscosity
Infill Density	0.14	Affects structural stiffness and PI
Raster Angle	0.11	Governs anisotropy and crack-path behavior
Layer Height	0.09	Directly controls PI and surface finish
Viscosity	0.07	Influences extrusion stability
Storage Modulus	0.05	Reflects melt elasticity
SiO_2 Loading	0.04	Contributes moderate reinforcement

reduction in complex viscosity. This behavior is advantageous in processes like FDM, where reduced viscosity at operational shear rates enhances extrudability while maintaining adequate melt strength for layer deposition.

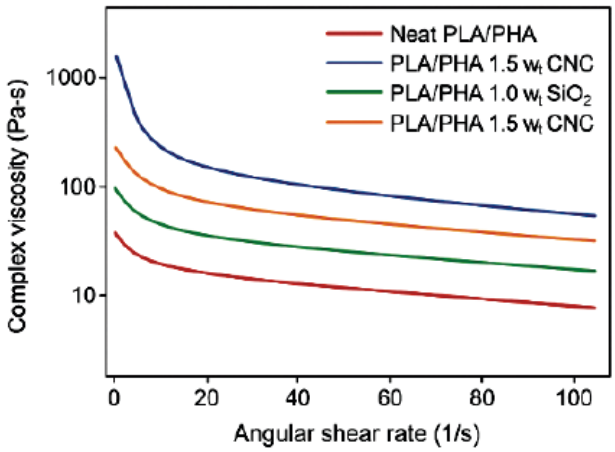

Figure 9: Complex viscosity (η) as a function of shear rate (or angular frequency), showing the characteristic shear-thinning behavior of the polymer melt.

Overall, the combined experimental, comparative, and validation results clearly demonstrate that machine learning-driven optimization is an effective strategy for enhancing the printability and strength of biodegradable polymer nanocomposites. The synergy between DOE-generated data, rigorous material characterization, and advanced ML modeling enabled precise prediction and optimization of composite behavior, establishing a scalable framework for intelligent biodegradable composite design.

4. CONCLUSION

This study successfully demonstrated a machine learning-driven optimization framework for improving the FDM printability and mechanical performance of biodegradable polymer nanocomposites based on PLA/PHA reinforced with CNC and SiO_2 nanofillers. The experimental results established that CNC provided superior mechanical reinforcement, achieving a maximum tensile strength of 54.1 MPa at 1.5 wt%, representing a 22.8% improvement over baseline PLA/PHA. SiO_2 offered moderate strength enhancement but exhibited superior extrudability at higher loadings. Rheological and thermal analyses confirmed that nanofillers influenced melt behavior and crystallization, which in turn governed print quality and interlayer bonding. While the present study demonstrates the strong potential of machine learning to accelerate the optimization of biodegradable polymer nanocomposites for FDM, it is important to acknowledge practical limitations associated with real-world implementation. The predictive performance of ML models is inherently dependent on the quality, diversity, and representativeness of the experimental dataset, and model generalizability may be affected by printer-to-printer variability, hardware-specific thermal control, and environmental conditions. Additionally, scaling such frameworks from laboratory-scale experimentation to industrial manufacturing requires the incorporation of larger, multi-source datasets and standardized calibration protocols. Consequently, machine learning should be regarded as a powerful decision-support tool that complements experimental insight rather than a universal replacement for process expertise. Future efforts integrating multi-printer data, in-situ sensing, and closed-loop control strategies will be essential to fully realize the practical impact of ML-driven optimization in sustainable additive manufacturing.

REFERENCES

[1] Dallaev, R., Papež, N., Allaham, M. M., & Holcman, V. (2025). Biodegradable polymers: properties, applications, and environmental impact. Polymers, 17(14), 1981. https://doi.org/10.3390/polym17141981

[2] Olonisakin, K., Mohanty, A. K., Thimmanagari, M., & Misra, M. (2025). Recent advances in biodegradable polymer blends and their biocomposites: a comprehensive review. Green Chemistry, 27(38), 11656-11704. https://doi.org/10.1039/D5GC01294E

[3] Guo, X., Liu, H., Nail, A., Meng, D., Zhu, L., Li, C., & Li, H. (2025). Design and Application of Stimuli-Responsive

Nanocomposite Hydrogels: A Review. Macromolecular Rapid Communications, 2401095. https://doi.org/10.1002/marc.202401095

[4] Paul, D. B., & Susila, P. A. (2025). Direct ink writing of bioceramic prosthetics and scaffolds: advances, challenges, and biomedical applications. Progress in Additive Manufacturing, 1-22. https://doi.org/10.1007/s40964-025-01002-x

[5] Antony Jose, S., Cowan, N., Davidson, M., Godina, G., Smith, I., Xin, J., & Menezes, P. L. (2025). A comprehensive review on cellulose Nanofibers, nanomaterials, and composites: Manufacturing, properties, and applications. Nanomaterials, 15(5), 356. https://doi.org/10.3390/nano15050356

[6] Ali, S., Mehra, V., Eltaggaz, A., Deiab, I., & Pervaiz, S. (2024). Optimization and prediction of additively manufactured PLA-PHA biodegradable polymer blend using TOPSIS and GA-ANN. Manufacturing Letters, 41, 795-802. https://doi.org/10.1016/j.mfglet.2024.09.099

[7] Jm, C. H., Narayanan, P., Pramanik, R., & Arockiarajan, A. (2025). Harnessing machine learning algorithms for the prediction and optimization of various properties of polylactic acid in biomedical use: a comprehensive review. Biomedical Materials.

[8] Verma, D., Dong, Y., Sharma, M., & Chaudhary, A. K. (2022). Advanced processing of 3D printed biocomposite materials using artificial intelligence. Materials and Manufacturing Processes, 37(5), 518-538. https://doi.org/10.1080/10426914.2021.1945090

[9] Baskaran, R., & T, T. (2025). Advances in Sustainable Polymeric Materials Derived from Renewable Biopolymers Integrated with Nanotechnology for Active Food Preservation: A Review. Polymer-Plastics Technology and Materials, 1-40. https://doi.org/10.1080/25740881.2025.2592713

[10] Terzopoulou, P., Achilias, D. S., & Vouvoudi, E. C. (2025). Advanced Wood Composites with Recyclable or Biodegradable Polymers Embedded—A Review of Current Trends. Journal of Composites Science, 9(8), 415. https://doi.org/10.3390/jcs9080415

[11] Radu, I. C., Vadureanu, A. M., Cozorici, D. E., Blanzeanu, E., & Zaharia, C. (2025). Advancing Sustainability in Modern Polymer Processing: Strategies for Waste Resource Recovery and Circular Economy Integration. Polymers, 17(4), 522. https://doi.org/10.3390/polym17040522

[12] Peng, B., Qi, X., Qiao, L., Lu, J., Qian, Z., Wu, C., ... & Kou, X. (2025). Nanocomposite-Enabled Next-Generation Food Packaging: A Comprehensive Review on Advanced Preparation Methods, Functional Properties, Preservation Applications, and Safety Considerations. Foods, 14(21), 3688. https://doi.org/10.3390/foods14213688

[13] Hussain, I., Ching, K. B., Uttraphan, C., Tay, K. G., & Noor, A. (2025). Evaluating machine learning algorithms for energy consumption prediction in electric vehicles: A comparative study. Scientific Reports, 15(1), 16124. https://doi.org/10.1038/s41598-025-94946-7

[14] Yoshi, A. M., Rohan, A., Mitu, S. A., Rabbi, M. M. K., Akther, S., & Ahmed, K. R. (2025). Real-Time Dynamic Pricing Using Machine Learning: Integrating Customer Sentiment and Predictive Models for E-Commerce. International Journal of Advanced Computer Science & Applications, 16(9). https://doi.org/10.14569/IJACSA.2025.0160904

[15] Alnemari, A. M., Elmessery, W. M., Qazaq, A. S., Moustapha, M. E., Rakhimgaliyeva, S., Abuhussein, M. F., ... & Elwakeel, A. E. (2025). Developing highly accurate machine learning models for optimizing water quality management decisions in tilapia aquaculture. Scientific Reports, 15(1), 35600. https://doi.org/10.1038/s41598-025-16939-w

[16] Karuppusamy, M., Thirumalaisamy, R., Palanisamy, S., Nagamalai, S., Massoud, E. E. S., & Ayrilmis, N. (2025). A review of machine learning applications in polymer composites: advancements, challenges, and future prospects. Journal of Materials Chemistry A. https://doi.org/10.1039/D5TA00982K

[17] Mehta, A., Vasudev, H., Prakash, C., Pramanik, A., Basak, A., & Shankar, S. (2025). State of the art in machine learning for the purpose of optimizing and predicting the properties of polymeric nanocomposites. Nanocomposite Manufacturing Technologies, 549-573. https://doi.org/10.1016/B978-0-12-824329-9.00016-4

[18] Malashin, I., Martysyuk, D., Tynchenko, V., Gantimurov, A., Nelyub, V., Borodulin, A., & Galinovsky, A. (2025). Machine Learning in Polymeric Technical Textiles: A Review. Polymers, 17(9), 1172. https://doi.org/10.3390/polym17091172

[19] Jalaee, A. (2025). Advanced polymeric and wood-derived composites: structure, processing, and application (Doctoral dissertation, University of British Columbia).

[20] Ho, M., Ramirez, A. B., Akbarnia, N., Croiset, E., Prince, E., Fuller, G. G., & Kamkar, M. (2025). Direct Ink Writing of Conductive Hydrogels. Advanced Functional Materials, 35(22), 2415507. https://doi.org/10.1002/adfm.202415507

[21] Gholap, A. D., Said, R. P., Khuspe, P. R., Pardeshi, S. R., Pingale, P. L., Bhandari, K. M., ... & Giram, P. S. (2025). Recent Advances in Polyurethane Polymer for Biomedical Applications. Molecular Pharmaceutics. https://doi.org/10.1021/acs.molpharmaceut.5c00538

[22] Pang, R., Lai, M. K., Teo, H. H., & Yap, T. C. (2025). Influence of Temperature on Interlayer Adhesion and Structural Integrity in Material Extrusion: A Comprehensive Review. Journal of Manufacturing and Materials Processing, 9(6), 196. https://doi.org/10.3390/jmmp9060196

[23] Arunprasand, T. R., & Nallasamy, P. (2025). Advancements in optimizing mechanical performance of 3d printed polymer matrix composites via microstructural refinement and processing enhancements: A comprehensive review. Mechanics of Advanced Materials and Structures, 32(22), 5616-5634. https://doi.org/10.1080/15376494.2024.2426776

[24] Petousis, M., Nasikas, N. K., Papadakis, V., Valsamos, I., Gkagkanatsiou, K., Mountakis, N., ... & Vidakis, N. (2025). Printability and Performance Metrics of New-Generation Multifunctional PMMA/Antibacterial Blend Nanocomposites in MEX Additive Manufacturing. Polymers, 17(3), 410. https://doi.org/10.3390/polym17030410

https://doi.org/10.12974/2311-8717.2025.13.12